ELSEVIER

Biophysical Chemistry 95 (2002) 7–22

Biophysical Chemistry

www.elsevier.com/locate/bpc

Lateral distribution of cholesterol in membranes probed by means of a pyrene-labelled cholesterol: effects of acyl chain unsaturation

B. Lagane[a], S. Mazères[a], C. Le Grimellec[b], L. Cézanne[a], A. Lopez[a,*]

[a]*Institut de Pharmacologie et de Biologie Structurale du CNRS, 205 route de Narbonne, 31077 Toulouse cedex 4, France*
[b]*Centre de Biochimie Structurale, INSERM U414, Université Montpellier I, 34093 Montpellier cedex 5, France*

Received 17 July 2001; received in revised form 28 September 2001; accepted 5 October 2001

Abstract

The lateral distribution of cholesterol in membranes in the fluid state was investigated by studying the variation of the molar absorption coefficient of pyrene-labelled cholesterol (Py-chol) vs. its concentration in vesicles made of phosphatidylcholine, with variable acyl chain unsaturations. Absorption measurements indicated non-ideal mixing of Py-chol in unsaturated lipids, a process mainly controlled by the cholesterol moiety of the probe. Similar abilities of cholesterol and Py-chol in perturbing the phase properties of pure saturated phosphatidylcholine were observed by DSC experiments. Immiscibility of sterols was corroborated by fluorescence polarization measurements, which indicated a weaker ordering effect of cholesterol in unsaturated membranes. The sizes and the quantities of sterol oligomers formed were calculated. A model for the lateral distribution of cholesterol in membranes is proposed and is applied to known cholesterol/phosphatidylcholine phase diagrams. Finally, the results are discussed with regard to recent models of biological membrane organization, (i.e. rafts).

Keywords: Liquid ordered domains; Absorption spectroscopy; Immiscibility; Self-association; Isodesmic model

1. Introduction

Recent advances dealing with the structure and organization of biological membranes suggest the existence of fluid-phase immiscibilities of biological interest [1–3]. Detergent insoluble domains (i.e. rafts) have been implicated in the regulation of numerous biological functions [4] including signal transduction events, sorting of membrane lipids and proteins, cellular trafficking and some pathological disorders. Detergent insolubility is a well-described property of tightly packed lipid assemblies [5,6]. Close correlation, arisen from studies based on Triton X100 (TX-100) insolubility, has been found between the presence of lipids with saturated acyl chains (as sphingolipid like species) and cholesterol in membranes, and the occurrence of those domains [1,7]. In contrast, most of the unsaturated cellular phospholipids were found to be soluble. Cholesterol and saturated lipids are known to form liquid ordered phases (L_o) when mixed in model membranes [8–12]. The enrichment of detergent insoluble membranes

* Corresponding author. Tel: +33-5-6117-5945; fax: +33-5-6117-5994.
E-mail address: lopez@ipbs.fr (A. Lopez).

0301-4622/02/$ - see front matter
PII: S0301-4622(01)00235-6

from cells in sphingomyelin, gangliosides and cholesterol [13] gave rise to the proposal that similar ordered domains might exist in biological membranes. To support this assumption, recent works clearly evidenced similar physical properties of detergent insoluble membranes isolated from mammalian cells and those of L_o states from model membranes [14,15]. With respect to the likely occurrence of ordered domains in biological membranes, additional insights came from studies focusing on the interactions and forces controlling their formation.

Previous studies of the phase behavior of binary mixtures containing cholesterol and phospholipids indicated non-ideal mixing of cholesterol and the presence of liquid-disordered/liquid-ordered immiscibility regions [8–12]. They described the L_o phases as cholesterol-enriched domains exhibiting intermediate physical properties between the solid-ordered and liquid-disordered phases, as revealed by both fast translational diffusion and highly ordered acyl chains. From monolayer experiments, as well as theoretical considerations, the non-ideal mixing of cholesterol has recently been described in terms of the formation of immiscible liquid cholesterol-phospholipid condensed complexes [16,17]. The use of ternary mixtures, which are thought to mimic biological membranes more closely than the binary ones when mixed saturated and unsaturated lipids coexist with cholesterol, gave further support for the occurrence of fluid–fluid immiscibilities [1,18–20]. Additionally, it was found that cholesterol can promote formation of L_o domains [1,19,21] when unsaturated and saturated lipids were mixed [22]. Both the nature of their head-group [9,23,24] and the structure of their acyl chains affect the interactions of cholesterol with lipids [26]. As is discussed in this article, modifying the degree of acyl chain saturation was also observed to cause great changes in cholesterol distribution and membrane dynamics. Kusumi et al., analyzing the effect of cholesterol on the dynamic properties of either saturated or *cis*-unsaturated membranes in the fluid state, labelled by cholesterol or phospholipid analogue spin probes [26–29], observed in 1,2-dioleoyl-*sn*-glycero-3-phosphocholine (DOPC) membranes that cholesterol was found to be inefficient in altering the motion of spin-labelled phospholipids. In contrast with this result, rotational diffusion of steroid probes decreased (although to a lesser extent than in saturated membranes) upon addition of cholesterol to unsaturated membranes. Altogether, the results were interpreted in terms of the immiscibility of cholesterol in membranes composed of *cis*-unsaturated lipid species due to the steric non-conformability between its rigid fused-ring structure and acyl chains bearing *cis*-unsaturations. Similar conclusions came from other studies [30–32]. Recent monolayer phase diagrams [16,33] also emphasized the lack of evidence for cholesterol complex formation with unsaturated phosphatidylcholines. This suggested increased free cholesterol concentration, (i.e. cholesterol not implicated in cholesterol-phospholipid interactions) when mixed with these lipids in membranes [16]. As the cholesterol is excluded from unsaturated environments, formation of cholesterol oligomers is then expected. Using saturation–recovery electron spin resonance techniques, the structure of cholesterol oligomers was further investigated [29]. The results obtained were then interpreted in terms of the presence of cholesterol-segregated domains of small size and/or of short lifetime (1–100 ns).

To get further insight into the molecular bases controlling the lateral distribution of cholesterol in membranes and to describe cholesterol-enriched domains accurately, the present work deals with the self-associative behavior of 1-pyrenemethyl-3β-hydroxy-22,23bisnor-5cholenate (Py-chol) in LUVs composed of 1,2-dimyristoyl-*sn*-glycero-3-phosphocholine (DMPC), egg yolk L-α-phosphatidylcholine (EPC) or DOPC in the fluid phase. The lateral distribution of this probe was investigated by means of absorption spectroscopy, as previously described [34,35]. The correct interpretation of data was obtained with classical models of the self-associative processes [34]. Comparisons with the lateral distribution of 1-hexadecanoyl-2-(1-pyrenedecanoyl)-*sn*-glycero-3- phosphocholine (Py-PC) or 1-hexadecanoyl-2-(1-pyrenedecanoyl)-*sn*-glycero-3-phosphoglycerol (Py-PG) in large unilamellar vesicles (LUVs) composed of EPC indicated that the self-association, and therefore the lateral distribution, of Py-chol are essentially

due to its cholesterol moiety. The results are in agreement with the formation of sterol-enriched domains depending on the degree of phospholipid acyl chain unsaturations. The size and the molar fractions of generated sterol-enriched domains were characterized. Taken together with differential scanning calorimetry (DSC) experiments demonstrating similar abilities of Py-chol and cholesterol in modulating the physical properties of bilayers composed of 1,2-dipalmitoyl-*sn*-glycero-3-phosphocholine (DPPC), this suggests the usefulness of Py-chol for probing the behavior of cholesterol in membranes in the fluid state. Finally, a model for the lateral distribution of cholesterol in membranes is proposed. It accounts for the distribution of L_o and liquid disordered lipid phase (L_α) phases in cholesterol /phosphatidylcholine phase diagrams [11,36]. This new view of lateral distribution of cholesterol is discussed with regard to recent models of biological membrane organizations, (i.e. rafts).

2. Materials and methods

2.1. Materials

DMPC (diC14:0PC) and DOPC (diC18:1PC) were purchased from Avanti Polar Lipids (Alabaster, AL, USA). DPPC, cholesterol and EPC, with a fatty acid distribution corresponding to C16:0 (34%), C18:0 (11%), C18:1 (31%) and C18:2 (18%), were obtained from Sigma (St Louis, MO, USA). Py-PC, Py-PG, Py-chol and 2-(3-(diphenylhexatriene)propanoyl)-1-hexadecanoyl-sn-glycero-β-phosphocholine (β-DPH-HPC) were purchased from Molecular Probes Inc. (Eugene, Oregon, USA). The purity of compounds was confirmed by thin-layer chromatography on silica-gel (Merck, Darmstadt, Germany) using chloroform/methanol/water (65:25:4, v/v) or petroleum ether/ether (70/30, v/v) as elution solvents for phospholipids and sterols, respectively. Solvents were of analytical grade. Chloroform/methanol solutions of phospholipids (9:1, v/v) or sterols (99:1, v/v) were stored at 4 °C before use. The concentration of phospholipid solutions was determined by both gravimetry (using a Sartorius super micro-balance) and phosphate titration [37]. With respect to cholesterol, a colorimetric method (Roche Molecular Biochemicals) was used.

2.2. Vesicle preparations

Lipids were mixed in chloroform/methanol solutions. The solvents were first removed under nitrogen and the mixtures were then further dried for 3 h under vacuum (1 torr). Dried samples were rehydrated in 2 ml Ca^{2+} and Mg^{2+} free phosphate buffer saline, pH 7.4 with NaN_3 0.2% (w/v). With respect to absorption spectroscopy measurements, this led to lipid final concentrations ranging from 10^{-4} M to 10^{-3} M, depending on the extent of added probes (see Fig. 2). In this respect and due to low incorporation rates no more than 7 mol% Py-chol were added to lipids in the experiments described below. Fluorescence polarization experiments were performed at a 10^{-5} M final lipid concentration including 1 mol% of β-DPH-HPC. Dispersed lipids were then vortexed for 1 min and sonicated for 10 min with an immersed tip at temperatures above the gel to liquid phase transition temperature (T_m) of lipids used (DOPC and EPC at room temperature and DMPC at 30 °C). The small unilamellar vesicles (SUVs) obtained using this procedure were kept overnight at 4 °C. Vesicle–vesicle fusion occurred, which yielded, in equilibrium, completely relaxed LUVs with diameters ranging between 100 and 150 nm as determined using photon correlation spectroscopy (model N4MD, Coulter, USA). The vesicles were then used no more than 1 or 2 days after their preparation.

2.3. Differential scanning calorimetry experiments

Vesicles composed of DPPC and either cholesterol or Py-chol were examined with the differential scanning calorimeter MC-1 instrument. 700 μl of a dispersion of vesicles was sealed into a sample pan and scanned twice at a rate of 0.5 °C/min from 20 °C to 60 °C.

2.4. Absorption spectroscopy measurements

Absorption spectra were performed with both Perkin Elmer UV/VIS Lambda 16 or Kontron

spectrophotometer UVICON 923 spectrometers at 26 °C using a 1-cm path length quartz cuvette. Calibration at a zero baseline was carried out taking air as the reference. Absorption spectra were then initially recorded between 650 and 280 nm in order to estimate absorption due to light scattering of LUV suspensions. Accordingly, removing the light scattering response by graphic deconvolutions of spectra [34] between 290 and 400 nm enabled us to obtain the optical density of pyrene-labelled lipids. Measurements and deconvolutions were performed twice for each sample and the mean value for ε was calculated. Finally, the data points shown in Fig. 2 correspond to determinations carried out with independent lipid mixtures.

2.5. Computer calculations

Calculations were performed using a non-linear least-squares package already described [34]. The confidence intervals for the estimated parameters corresponded to an error risk of 5%.

2.6. Fluorescence polarization measurements

Experiments were carried out using a thermostated T-format apparatus. β-DPH-HPC was used as the probe. The excitation wavelength was 360 nm, and fluorescence was measured over the wavelength range of 400–500 nm. The polarization P is expressed as $P=(I_{II}-I_{\perp})/(I_{II}+I_{\perp})$.

3. Results and discussion

3.1. The effect of Py-chol on phospholipid phase behavior

To confirm the suitability of this probe for mimicking the behavior of cholesterol in membranes and that the lateral distribution of Py-chol is mainly dominated by its cholesterol moiety, it was of interest to investigate the effect of Py-chol on the physical properties of lipids. DSC has been used extensively to study the effects of cholesterol on lipid phase transitions [12,25]. The comparison of Fig. 1a and Fig. 1b, in the range of Py-chol solubility in phospholipid membranes (0 to 7%), show that Py-chol was as efficient as cholesterol, both in decreasing the enthalpy of the main transition and in inhibiting the pretransition. Accordingly, this indicates that Py-chol/phospholipid interactions are likely to be controlled by the cholesterol moiety of the probe.

3.2. Absorption measurements

To determine the lateral distribution of pyrene-labelled lipids in the ground state in LUVs containing phosphatidylcholines in the fluid state, measurements of their molar extinction coefficients ε (ε_{meas}) corresponding to the allowed $S_0 \rightarrow S_2$ transitions [38] as a function of the probe to host lipid molar ratios were performed. Varying the extent of added Py-chol was carried out within LUVs composed of phosphatidylcholines with increased degrees of acyl chain unsaturations, namely DMPC, EPC and DOPC. The behavior of Py-PC and Py-PG in EPC was also investigated. As shown in Fig. 2, values averaging 35 000 $M^{-1}\,cm^{-1}$ were measured at 2 mol% added probes and were found to remain unchanged upon an increase in the probe molar fraction. This was observed with respect to all mixtures studied. In contrast, the ε values appeared to change markedly as the probe concentrations were diluted. Both hypochromic and hyperchromic effects were detected upon dilution of probes depending as first assumption, on the labelled molecule used. Decreasing the Py-chol content in membranes composed of phosphatidylcholines yielded increased values for ε. This was observed more sharply in membranes composed of unsaturated species, (i.e. DOPC). In contrast, the molar extinction coefficients for pyrene-labelled phospholipids were found to slightly decrease upon their dilution in vesicles made of EPC. Following these experiments, no shift with respect to maximum wavelengths of pyrene absorption bands was detected (not shown). Similar dependence upon dilution of anthracene or pyrene-labelled lipids in bilayers has previously been observed [34,35].

Hypochromism of poly (1-vinylpyrene) in tetrahydrofurane (THF) solutions has also been reported [39]. In contrast, these authors found unchanged absorption properties of 1-pentylpyrene

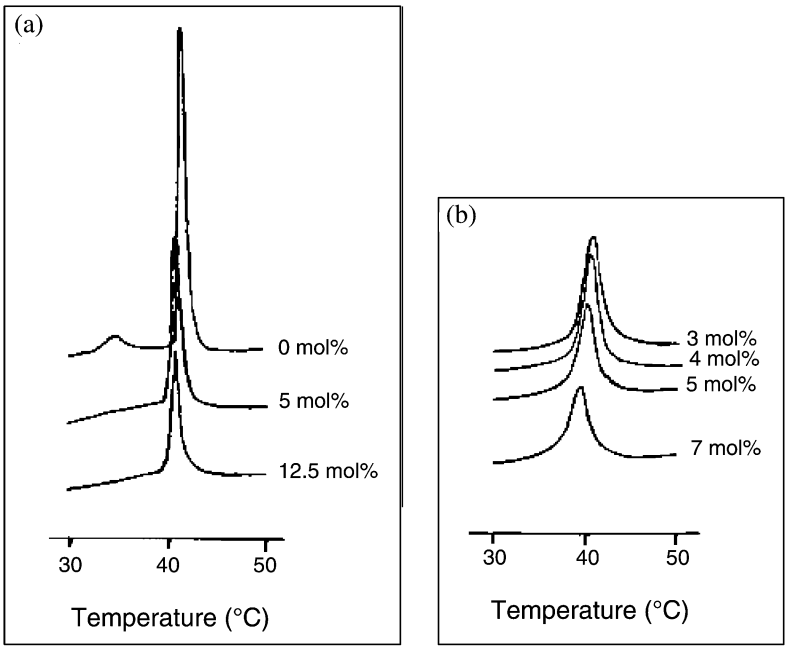

Fig. 1. Calorimetric scans for DPPC/cholesterol (a) and DPPC/Py-chol (b) as a function of molar fractions of incorporated sterols.

at similar concentrations in THF. According to ^{1}H-NMR data, these UV absorption measurements were adequately interpreted, assuming a high interaction between pyrenyl groups in the polymeric environment. Similar arguments emerge from our experiments. Diluting pyrene labelled phospholipids and Py-chol in ethanol and methanol respectively from 10^{-4} to 10^{-7} M were found to be inefficient in altering the measured molar extinction coefficients, in contrast to what was observed in membranes [35]. Accordingly, one can assume that anisotropic constraints in membranes can lead to interactions between probes. An overlapping of π molecular orbitals is therefore likely to take place, thereby changing the absorption properties of interacting chromophores as shown in Fig. 2. However, to our knowledge, no strict explanation predicting the changes in ε values upon modification of the probe concentration is available. Fig. 2 shows either the hypochromic or the hyperchromic effects, depending on both the probe/lipid mixtures used and the characteristics of interactions involved between probes. This was confirmed in recent work, emphasizing increased values of molar extinction coefficients for Py-PC and Py-PG upon decreasing the probe to host lipid molar ratios in vesicles composed of glycolipids [35]. Discrepancies were also observed with respect to the measured absorption properties at large dilutions of probes in membranes (where no interactions between probes are expected to occur). We assume this observation depends firstly on the pyrene-labelled molecule used as demonstrated by distinct properties of pyrene-labelled phospholipids and cholesterol in bilayers made of EPC. Additionally the structure of the host lipid used is also of importance. If compared in either saturated (DMPC) or unsaturated (DOPC) bilayers, the ε values for Py-chol showed a 2.5-fold increase in the unsaturated ones. Investigations have reported the variations of polarity across membrane bilayers according to acyl chain unsaturations [40]. Accordingly, one can assume that the allowed $S_0 \rightarrow S_2$ transitions depend on the polarity of membranes. In contrast to what was previously argued [41], the ε values for various pyrene-labelled lipids in organic solutions were found to vary according to the organic solvent used [35]. This strongly sug-

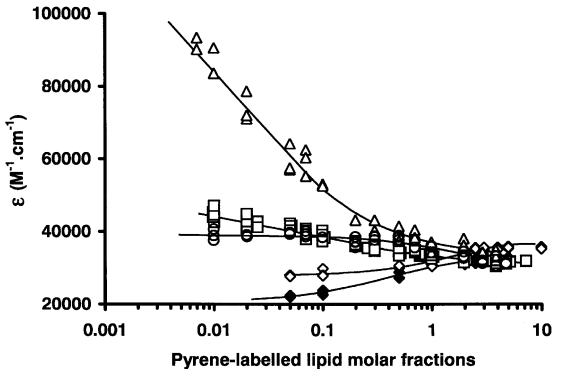

Fig. 2. The effect of the degree of acyl chain unsaturation on the variations of molar extinction coefficients ε at 343 nm for Py-chol upon varying its molar fraction in LUVs composed of phosphatidylcholines — Comparison with the behavior of pyrene-labelled phospholipids (Py-PC and Py-PG). Fitting curves according to the isodesmic model are also shown and are calculated according to the values indicated in Table 1. For the sake of clarity, only 30 ε values out of 54 and 94 independent determinations are shown for Py-chol and Py-PC in EPC, respectively. The symbols used are the following: EPC/Py-PC, filled diamond; EPC/Py-PG, open diamond; EPC/Py-chol, open square; DMPC/Py-chol, open circle; DOPC/Py-chol, open triangle; fitting curves (continuous black line).

gests that the measured molar extinction coefficients of probes (in addition to interactions between probes) also depend on the structure of lipid bilayers used.

3.3. Self-association of Py-chol in membranes

Interpretations of the above data were carried out according to the self-associative isodesmic model, as described in 5. [34]. Fitting curves, correlating the calculated values for ε (ε_{calc} as a function of C_t, ε_{mono}, ε_{ext}, ε_{int} and K) with the experimental results are shown in Fig. 2. The solution values for the above parameters are indicated in Table 1. As expected, note that the ε_{mono} values are nearly identical to the measured ones at large dilution. This emphasizes the coherence of our analytical approach and confirms that few interactions between probes exist at low probe/host lipid molar ratios. The self-association process leads to the formation of oligomers (*n*-mers) whose distribution and size, as a function of probe molar fractions, are calculated according to Eqs. (A4) and (A5) and are shown in Fig. 3a–d with the corresponding association constants *K*, reported in Table 1. For the sake of clarity, only *n*-mers up to pentamers are presented. However, it is clear that both their size and molar fractions depend on

Table 1
Characteristics of the association constant *K* and molar extinction coefficients (ε_{mono}, ε_{ext} and ε_{int}) for pyrene labelled phospholipids (Py-PC and Py-PG) and cholesterol (Py-chol) in LUV composed of various phosphatidylcholines

Lipid/probe mixture	ε measured at large dilution ($M^{-1}\cdot cm^{-1}$) ±S.D.	*K* (M^{-1}) ±S.D.	ε_{mono} ($M^{-1}\cdot cm^{-1}$) ±S.D.	ε_{int} ($M^{-1}\cdot cm^{-1}$) ±S.D.	ε_{ext} ($M^{-1}\cdot cm^{-1}$) ±S.D.	S.D. number of data
EPC/PyPG	27 800 ±600	0.12 ±0.05	27 707 ±650	20 220 ±400	32 821 ±1200	1.82% 28 pts
EPC/PyPC	22 200 ±700	0.97 ±0.09	20 659 ±600	30 398 ±1200	38 058 ±1500	1.78% 94 pts
EPC/Py-chol	45 300 ±2000	872.05 ±223	46 276 ±1580	30 355 ±980	34 275 ±1100	0.9% 54 pts
DOPC/Py-chol	90 200 ±5000	2771.41 ±299	109 315 ±3500	32 265 ±3500	40 719 ±4000	3.25% 53 pts
DMPC/Py-chol	38 900 ±1250	42.63 ±10	39 086 ±1250	19 777 ±5100	32 761 ±3400	1.42% 39 pts

The parameter confidence intervals (S.D.) are calculated for a 5% error risk. The molar extinction coefficients measured at large dilution are those calculated using the most diluted samples, shown in Fig. 2.

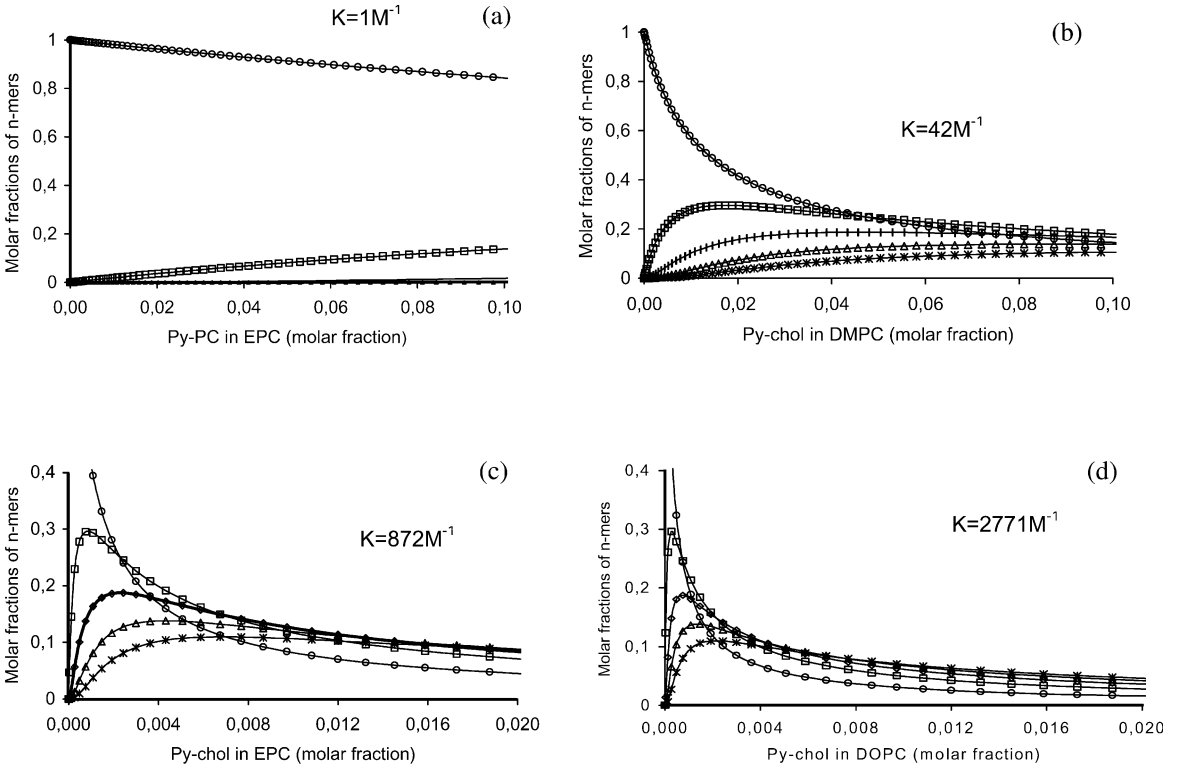

Fig. 3. Calculated *n*-mer distributions up to pentamers for Py-PC (a) and Py-chol (b–d) upon varying their molar fractions in LUVs composed of phosphatidylcholines. The calculations were performed according to Rodriguez et al. [34], using the appropriate values for *K* indicated in Table 1. The symbols used are the following: Monomers (circles); dimers (squares); trimers (diamonds); tetramers (triangles); pentamers (crosses).

the amount of probes incorporated. The following additional conclusions emerge from the above data. (i) Regarding LUVs composed of EPC, large discrepancies were found with respect to the self-association of the pyrene-labelled phospholipids Py-PC (Fig. 3a and Table 1), Py-PG (Table 1) and Py-chol (Fig. 3c and Table 1). Much weaker self-association constants were observed for Py-PC and Py-PG (with *K* values lower than 1 M^{-1}). As a consequence, Py-PC (Fig. 3a) and Py-PG [35] primarily exist as monomers in EPC bilayers. In contrast, the *K* values for Py-chol in EPC vesicles were found to be 872 times greater. This gives rise to the occurrence of molecular stacks, (i.e. *n*-mers) even at low incorporation ratios (at 2 mol% Py-chol, molar fractions close to 0.05 for the free monomer form are observed in Fig. 4). Accordingly, and with respect to the weak self-associative behavior of phospholipids labelled with pyrene in bilayers composed of EPC, one can then assume that the self-association, and therefore the lateral distribution, of Py-chol in EPC bilayers are essentially due to its cholesterol (rather than its pyrenyl) moiety. This correlates well with previous electron spin resonance data, suggesting non-ideal mixing of cholesterol in EPC bilayers [26] and the formation of cholesterol rich-clusters in 1-palmitoyl-2-oleoyl-*sn*-glycero-3-phosphocholine (POPC) model membranes [30].

(ii) It is seen from Fig. 3b–d that the estimated association constants for Py-chol increase following introduction of unsaturations in the acyl chains of host lipids. Accordingly, the *K* values increase in the order DMPC < EPC < DOPC. Even though Py-chol tends to self-associate in any bilayer used, these results strongly suggest higher immiscibility

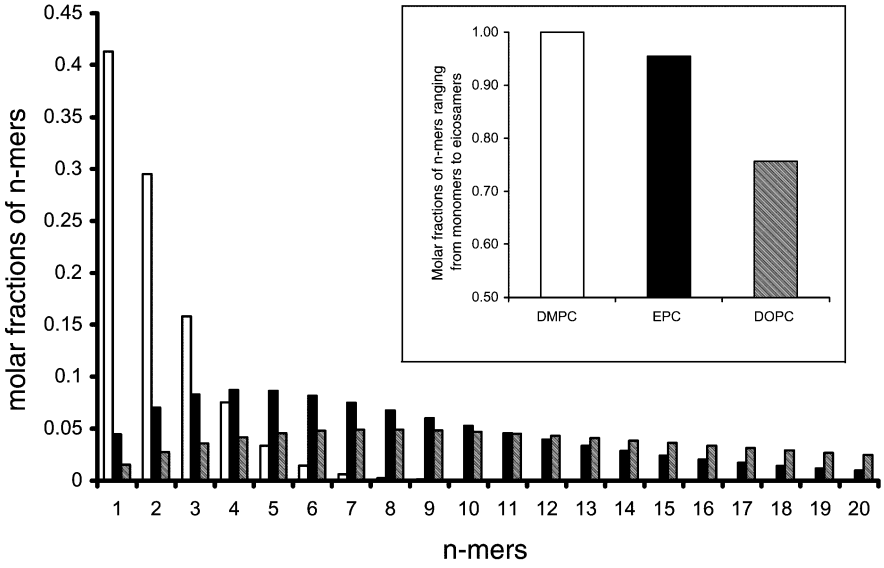

Fig. 4. Calculated *n*-mer distributions for Py-chol from $n=1$ to $n=20$, at 2 mol% Py-chol in DMPC (open bars), EPC (black bars) and DOPC (grey bars) LUVs. Insert: total sum of molar fractions of Py-chol *n*-mers ranging from monomers to eicosamers at 2 mol% Py-chol in DMPC, EPC or DOPC bilayers.

of Py-chol molecules in unsaturated (or higher miscibility of Py-chol in saturated) fluid phases. This is shown by larger amounts of Py-chol oligomers from DMPC to DOPC bilayers (Fig. 3b–d). Additionally, as shown in Fig. 3, the occurrence of Py-chol oligomers of larger size increased with the unsaturation degree (DMPC < EPC < DOPC), at a given probe molar fraction. The addition of molar fractions of *n*-mers ranging from monomers up to eicosamers in the above-cited bilayers was performed at 2 mol% added Py-chol, as mentioned in the insert of Fig. 4. In contrast to that observed with respect to DMPC bilayers (and to a lesser extent with EPC bilayers), one can see that oligomers composed of more than 20 Py-chol molecules are still present in large amounts (approximately 25%, insert of Fig. 4) in DOPC bilayers at this, rather low, probe molar fraction.

(iii) If compared with the lateral distribution of pyrene-labelled phospholipids, it is likely that the formation of Py-chol oligomers in either PC bilayers accounts for favored cholesterol/cholesterol interactions in membranes. Thus, except at very low cholesterol concentrations, ideal mixing of cholesterol with lipids seems unlikely. Similar conclusions have been reported previously [28,31]. Our results also agree well with stronger immiscibility of Py-chol in the unsaturated membranes rather than in the saturated ones. One can then assume preferential interactions of the cholesterol moiety of Py-chol with the DMPC, rather than with the DOPC (or EPC) molecules. If compared with the lateral distribution of cholesterol in *cis*-unsaturated bilayers, higher miscibility of cholesterol in *trans*-unsaturated phospholipids has been reported [29]. Thus, unfavorable interactions as a result of steric hindrances of the rigid cholesterol moiety of Py-chol with the *cis* double bonds of unsaturated lipids are likely to take place in EPC and DOPC bilayers.

3.4. The ordering effect of cholesterol in unsaturated membranes

Correlations have been reported between the ability of sterols to interact strongly with saturated lipids and to pack them tightly [24]. Accordingly, one can assume that large immiscibility of Py-chol in unsaturated membranes, as a result of restricted interactions of its cholesterol moiety with phos-

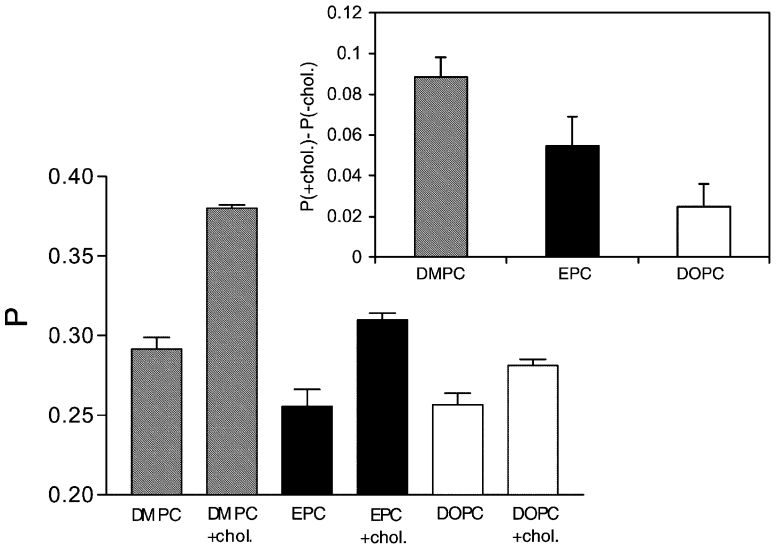

Fig. 5. Steady state fluorescence polarization of β-DPH-HPC in samples containing 1 mol% β-DPH-HPC incorporated in LUVs composed of DMPC, EPC or DOPC with or without 30 mol% cholesterol. For the sake of clarity, only the measurements at 26 °C are shown (but the experiments were carried out at temperatures ranging from 15 to 37 °C). The results are the mean results for two independent experiments with corresponding S.D. Insert: ordering effect induced by 30 mol% cholesterol in the above mentioned bilayers as revealed by the following subtraction: P (with 30 mol% cholesterol) $-$ P (without 30 mol% cholesterol).

pholipids and/or favored cholesterol/cholesterol interactions would correlate with diminished abilities of cholesterol in ordering lipid bilayers. To test this hypothesis, the magnitude of fluorescence polarization rate of β-DPH-HPC was measured in LUVs containing 1 mol% β-DPH-HPC incorporated in DMPC, EPC or DOPC bilayers, with or without 30 mol% cholesterol (Fig. 5). Ordered lipid environments lead to restricted conformational and rotational motions of fluorophores and then higher rates of polarization are measured. The rate of β-DPH-HPC fluorescence polarization (P) measured at 26 °C in DMPC bilayers is related to the presence of the fluorophore in the L_α state (P close to 0.28). Significant increases in the polarization rate were observed upon addition of 30 mol% cholesterol (P close to 0.37). This reflects a strong ordering effect of cholesterol in DMPC bilayers as summarized in the insert of Fig. 5 [P (with 30 mol% cholesterol) $-$ P (without cholesterol) close to 0.09]. In contrast, increasing phospholipid unsaturation was found to decrease the ability of cholesterol in ordering acyl chains (Fig. 5). Thus, the fluorescence polarization rate of β-DPH-HPC reflecting the ordering effect upon addition of cholesterol, decreases in the order DMPC > EPC > DOPC.

Considered as a whole, the results emphasize the relationships between the miscibility of cholesterol in membranes and its ability to increase ordering of saturated PC chains as it was demonstrated besides clearly [42]. Low ordering effects of cholesterol in DOPC or EPC membranes reveal restricted sterol/lipid interactions. Immiscibility of cholesterol is therefore likely to take place as a result of preferential sterol/sterol (and/or diminished sterol/lipid) interactions in unsaturated membranes. This agrees well with the data from Figs. 3 and 4, showing the occurrence of numerous sterol oligomers of large size as the degree of unsaturations increases in membranes.

3.5. Organization of cholesterol-rich domains in membranes

In ternary mixtures containing cholesterol, with both saturated and unsaturated lipids, cholesterol is therefore expected to interact more readily with

the saturated rather than with the unsaturated lipid species. Ordered saturated lipids would coexist with disordered (less ordered) unsaturated lipids. As a result, this process is assumed to increase fluid phase immiscibilities, thereby leading to the coexistence of L_o and L_α domains. As evidence, the ability of various sterols to promote the formation of ordered domains in bilayers containing DPPC and an unsaturated lipid specie has been found to correlate with the ordering of saturated lipids and thereby, the enhancement of its immiscibility in a lipid bilayer in the L_α state [22]. In binary mixtures, the uneven distribution of cholesterol leads to the coexistence of cholesterol-rich and cholesterol-poor phases. As a consequence, L_o domains were found to coexist with L_α phases [8–12]. This process was found to strongly depend on both the cholesterol concentration and the structure of the lipid bilayer. In this respect, evidence came from comparative studies dealing with the occurrence of L_o phases in binary mixtures composed of cholesterol and either DMPC or POPC [11,36]. The distribution of the fluorescence lifetime of *trans*-parinaric acid was found to correlate with the coexistence of L_o and L_α phases from 7 to 40 mol% cholesterol in the unsaturated bilayers at 25 °C [11]. In contrast, the structure of DMPC bilayers containing more than 25–30 mol% cholesterol was reported to correspond to that of a L_o phase over a wide range of temperatures [11,36]. These gave support to a decreased ability of cholesterol to induce ordered domain formation in bilayers composed of unsaturated lipids where numerous cholesterol oligomers of large size are supposed to exist, as shown in our work. Additionally, both studies emphasized the disappearance of L_o phases and the prevalence of a L_α phase at cholesterol concentrations lower than 7 mol% cholesterol, thereby agreeing with previous studies showing the requirement for substantial amounts of cholesterol to promote the formation of ordered domains [8]. However, this contrasted with more recent high-sensitivity differential scanning calorimetry data relating to significantly lower cholesterol concentrations at which L_o phases first arise in DPPC bilayers [12].

3.5.1. Correlation between the cholesterol self-association and the amount of phospholipid in the L_o phase

A model taking the self-association of cholesterol into account, similar to that observed for Py-chol in our work, supposes the ordering of phospholipids that are around cholesterol oligomers or in contact with cholesterol monomers. We assumed cholesterol monomers and oligomers as circular areas characterized by their corresponding radius R_n, and their neighborhood composed of lipid molecules in all *trans* fully-extended conformations. Similar to the proposed influence of integral membrane proteins on the ordering of adjacent lipids [43–45], we assumed the behavior of the lipid order parameter away from cholesterol monomers or oligomers described by an exponential decay function with a coherence length ξ [46]. From compression isotherms at the air/water interface, we found cross-sectional areas for cholesterol to be slightly lower than those observed for Py-chol (45 Å^2/molecule) and equal to 39 Å^2/molecule at 20 mN/m (not shown) as previously described [47]. This led to the knowledge of radius R_n for individual n-mers $[R_n=(39\cdot n)/\pi)^{1/2}]$. Accordingly, the following expression of the area A_n of ordered phospholipids around an oligomer composed of n-stacked cholesterol molecules can be written:

$$A_n=\left[(R_n+\xi)^2\cdot\pi\right]-[39\cdot n] \quad (1)$$

Taking into account the molar fraction α_n of n-mers at given cholesterol to host lipid molar ratios (and deduced from distributions of Py-chol n-mers as those shown in Fig. 4), the area A^*_n of ordered phospholipids around α_n oligomers composed of n units in the bilayer results:

$$A^*_n=A_n\cdot\alpha_n \quad (2)$$

thereby leading to the following expression of the total area of ordered phospholipids in the bilayer:

$$A_{OL}=\sum_{i=1}^{i=n}A^*_n \quad (3)$$

The amounts of domains composed of ordered phospholipids $\langle A_{OL}\rangle$ in cholesterol/phospholipids binary mixtures are then expressed as the ratios

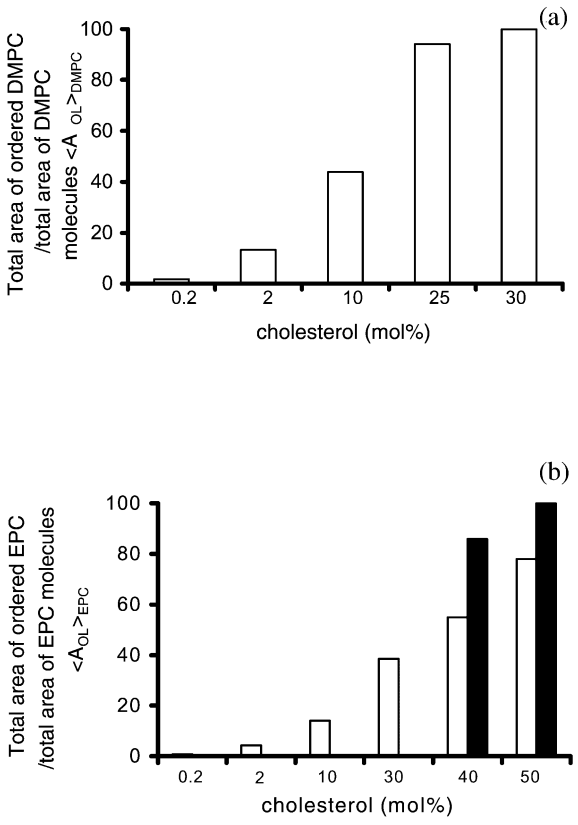

Fig. 6. Calculated areas of ordered phospholipids $\langle A_{OL}\rangle$ as a function of the molar fraction of cholesterol incorporated in DMPC (a) or EPC (b) bilayers. Calculations were performed according to equations 1–3, taking 12 Å (open bars) or 17 Å (filled bars) as values for ξ. For details, see text. Considering the uncertainty of the distribution values of *n*-mers and that of the area of the various lipids, the *Y* axis, uncertainty is of the order of $\pm 5\%$ of its extent.

between the total area A_{OL} of ordered phospholipids and the total area A_{DMPC} of DMPC $[\langle A_{OL}\rangle_{DMPC}]$ or A_{EPC} of EPC $[\langle A_{OL}\rangle_{EPC}]$ molecules, respectively.

3.5.2. Phase diagrams of DMPC or EPC and cholesterol self-association

Using that model, calculations were carried out to estimate, quantitatively, the presence of L_o domains in bilayers composed of DMPC and EPC as a function of the amount of added sterol molecules. The results obtained are shown in Fig. 6a (DMPC), Fig. 6b (EPC) and Fig. 7. In Fig. 6, the $\langle A_{OL}\rangle$ values (expressed as the percentages of ordered phospholipids) are shown as a function of cholesterol molar fractions (γ_{chol}). Deduced from Fig. 6 and shown in Fig. 7 are the efficiencies $E_{(chol)}$ of one mol% cholesterol to induce the formation of L_o domains ($E_{(chol)} = \langle A_{OL}\rangle / \gamma_{chol}$) as a function of cholesterol molar fractions.

Following the above calculations, 25–30 mol% cholesterol was found to alter the order of the whole of added DMPC molecules (Fig. 6a), according to values for ξ ranging from 11 to 13 Å. This agrees well with previous estimates for ξ between 10 and 20 Å [43,45], depending on both the system used and the temperature [44]. These results also strongly accord with the above mentioned works dealing with the phase behavior of mixtures containing DMPC and cholesterol [11,36] and showing the presence of a unique liquid ordered phase above 25–30 mol% cholesterol. Our model also correlates with works emphasizing the co-existence of cholesterol-enriched and cholesterol-poor liquid phases at intermediate cholesterol concentrations. However, ordered lipids were observed to coexist with the liquid crystalline L_α phase at rather low cholesterol concentrations, in contrast to what was postulated in the above mentioned works [8]. At 2 mol% cholesterol, the total area A_{OL} of ordered lipids still represents

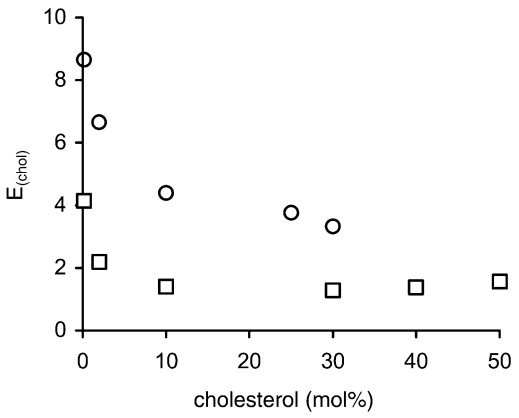

Fig. 7. Cholesterol efficiency $E_{(chol)}$ in promoting the formation of ordered phospholipids as a function of molar fractions of incorporated cholesterol in DMPC (circles) or EPC (squares) bilayers. The results are expressed as the percentages of ordered phospholipids by one mol% cholesterol.

approximately 10% of the total area of DMPC molecules in the bilayer. Agreeing with this result, broad and sharp components related to the presence of coexisting liquid ordered and disordered phases, respectively, have been observed from deconvolutions of the DSC endotherms of aqueous dispersions of DPPC containing 2 mol% cholesterol [12]. Everything taken into consideration, we assume that L_o phases are likely to exist at low cholesterol concentrations. To confirm this assumption, the efficiency $E_{(chol)}$ of 1 mol% cholesterol to order lipids was found to increase upon decreasing the cholesterol to host lipid molar ratios (Fig. 7). This accounts for the lower effect of cholesterol oligomers of large size than either those of small size or cholesterol monomers on the formation of ordered domains at high cholesterol concentrations.

The use of similar values for ξ (12 Å) was found to correlate with the coexistence of ordered and disordered lipids in EPC bilayers containing cholesterol concentrations as high as 50 mol% (Fig. 6b, open bars). Accordingly, this accounts for a lower ability of cholesterol to induce the formation of ordered domains in bilayers composed of EPC rather than DMPC molecules (Fig. 7). It is likely that this results from the occurrence of large amounts of cholesterol oligomers of larger size in unsaturated membranes and, if compared with that of monomers or small cholesterol oligomers, again emphasizes their diminished efficiency in promoting the formation of ordered domains. To confirm this assumption and as what was observed in DMPC bilayers (to a lesser extent however), the efficiency $E_{(chol)}$ of 1 mol% cholesterol to form ordered domains was observed to increase at low cholesterol to lipid molar ratios (Fig. 7) where both the size and the amount of oligomers are low. However, our results contrast with the publication of Reyes Mateo et al. [11], showing the presence of a unique L_o phase in POPC bilayers containing approximately 40 mol% cholesterol. To be precise and according to Eqs. (1)–(3), increased values for ξ ranging between 16 and 18 Å were required to account for the ordering of all phospholipid molecules in EPC bilayers containing 40–50 mol% cholesterol (see Fig. 6b, filled bars). However, if compared with DMPC/cholesterol mixtures, one can expect lower cholesterol/EPC mismatch, thereby leading to lower ξ values. Accordingly, one can assume that higher cholesterol immiscibility in EPC bilayers (and the occurrence of more cholesterol oligomers) is likely to account for the observed discrepancies between the ordering of phospholipids in bilayers composed of POPC [11] or EPC (our work) molecules.

4. Conclusions

The following conclusions emerge from this study: (i) DSC experiments indicated a comparable ability of cholesterol and Py-chol in decreasing the DPPC enthalpy transition and in suppressing the DPPC pretransition. Moreover, the comparison of absorption spectroscopy data between Py-chol and pyrene-labelled phospholipids indicated that a self-association of Py-chol was mainly dominated by its cholesterol moiety. These results agree with the suitability of using Py-chol to investigate the behavior of cholesterol in membranes in the fluid state. (ii) They also suggest that the lateral distribution of cholesterol depends strongly on phospholipid unsaturations in membranes. Even though Py-chol tends to self-associate in all phosphatidylcholine bilayers used in this study, non-ideal mixing was more readily observed in unsaturated bilayers, thereby leading to the formation of cholesterol-rich oligomers. The sizes and the molar fractions of generated cholesterol oligomers, depending on both the characteristics of the host lipid matrix used and the amount of sterol incorporated, are deduced. The formation of substantial amounts of oligomers of large size was described in unsaturated membranes or at high probe to host lipid molar ratios. (iii) Self-association of cholesterol in membranes as a result of weak sterol/phospholipid interactions was found to correlate with a decreased ability to order phospholipids, thereby explaining the lower ability of cholesterol to induce liquid-ordered phases in unsaturated membranes [11,45]. (iv) In mixtures composed of cholesterol with both saturated and unsaturated lipid species, (i.e. biological membranes), cholesterol is therefore assumed to interact more readily with the saturated lipids. As discussed in recent

work [41], this process is expected to preferentially order the saturated lipids, thereby increasing their immiscibility in a disordered unsaturated environment. The results presented are therefore consistent with models of biological membrane organization, suggesting the coexistence of unsaturated phospholipid-enriched domains with TX-100 insoluble ordered domains as lipid rafts, rich in saturated lipids [2,3,48]. Those domains were often described as cholesterol-enriched or cholesterol-poor domains. In this respect, note that our work does not exclude the presence of cholesterol in unsaturated liquid disordered domains, where cholesterol as oligomers is expected to reside. This study is of particular importance with regard to both the numerous biological functions of ordered domains [4] and the role of cholesterol in determining the activity of embedded proteins [49,50] in cell membranes.

5. Annexes

5.1. Annex 1: self-associative model

To analyze our results the formalism already described was applied [34]. Oligomers (called *n*-mers) of various size are supposed to result from the self-association, by stacking, of Py-chol probes. Assuming an infinite linear self-association scheme in which each step is characterized by the same equilibrium constant *K*, only three kinds of contributions are expected to account for the absorption properties [34]: the molar extinction coefficients of free monomers (ε_{mono}); and in a stack of *n*-mer, the contributions of both (*n*-2) internal (ε_{int}) and the two external (ε_{ext}) units. The calculated molar extinction coefficient ε_{calc} for a given probe concentration C_t is:

$$\varepsilon_{calc} = \alpha_{mono}\varepsilon_{mono} + \alpha_{ext}\varepsilon_{ext} + \alpha_{int}\varepsilon_{int} \quad (A1)$$

where α_{mono}, α_{ext} and α_{int} are the molar fractions of free monomers and those of probes at the extremities and inside the stacks, respectively. Applying mass conservation, we have:

$$C_t = \sum_{i=l}^{i=n} i\cdot[A_i] \quad (A2)$$

where $[A_i]$ is the molar concentration of *n*-mers consisting of *i* pyrene-derived molecules, corresponding to the molar fractions α_i, defined as:

$$\alpha_i = i\cdot[A_i]/C_t \quad (A3)$$

and where,

$$1 = \alpha_1 + \alpha_2 + \ldots + \alpha_i + \ldots + \alpha_n \quad (A4)$$

A relationship between C_t, $[A_1]$ and *K*, where $[A_1]$ is the monomer molar concentration can be found [34]. Accordingly the calculation of individual molar concentrations of *n*-mers is:

$$[A_i] = K^{i-1}\cdot[A_1]^i \quad (A5)$$

Knowing C_t and using the above equations, we were able to calculate, by an iterative process [34], both α_{mono}, α_{ext} and α_{int} and determine the best values for the different parameters *K*, ε_{mono}, ε_{ext} and ε_{int} shown in Table 1. According to Eqs. (A3), (A4) and (A5), this then led to descriptions of *n*-mer distributions as a function of the host lipid to probe molar ratios indicated in Fig. 3a–d.

5.2. Annex 2: expression of molar concentrations for pyrene-labelled lipids in bilayers

Modelling the self-associative behavior of Py-chol in the lipid bilayer was performed, taking into consideration the membrane thickness as a third dimension to calculate the molar concentrations C_t (in mol.l^{-1}) of probes. The following calculations are related to DMPC and taken as an example.

An average molecular area M_a equal to 60.2 Å^2/mol was chosen for DMPC [51] and a length (*L*) of 14.5 Å was estimated [52]. The volume V_p of one mole of DMPC was: $V_p = M_a\cdot L\cdot N$, where *N* is Avogadro's number. The density of a mole of DMPC is then obtained: $\rho = M_W/V_p = 1291$ g/l, where M_W is the DMPC molecular weight (M_W = 678 g/mol). This corresponds to a molar concentration C_m of DMPC ($C_{m(DMPC)}$) equal to 1.9 M ($C_m = 1/V_p$). Then, knowing the probe to host lipid molar ratio γ, the following expression of C_t was: $C_t = \gamma$, $C_m = \gamma\cdot\rho/M_W$.

Applying similar calculations, we found C_m values equal to 1.32 M and 1.28 M for EPC (with M_a = 66.4 Å^2/mol and *L* = 19 Å [53]) and DOPC

(with $M_a = 72.2$ Å^2/mol and $L = 18$ Å [54]), respectively.

Acknowledgments

This work was supported by the Association pour la Recherche contre le Cancer and the Centre National de la Recherche Scientifique.

References

[1] S.N. Ahmed, D.A. Brown, E. London, On the origin of sphingolipid/cholesterol-rich detergent-insoluble cell membranes: physiological concentrations of cholesterol and sphingolipid induce formation of a detergent-insoluble, liquid-ordered lipid phase in model membranes, Biochemistry 36 (1997) 10944–10953.

[2] D.A. Brown, E. London, Structure and origin of ordered lipid domains in biological membranes, J. Membr. Biol. 164 (1998) 103–114.

[3] A. Rietveld, K. Simons, The differential miscibility of lipids as the basis for the formation of functional membrane rafts, Biochim. Biophys. Acta 1376 (1998) 467–479.

[4] D.A. Brown, E. London, Functions of lipid rafts in biological membranes, Annu. Rev. Cell. Dev. Biol. 14 (1998) 111–136.

[5] S.K. Patra, A. Alonso, F.M. Goni, Detergent solubilisation of phospholipid bilayers in the gel state: the role of polar and hydrophobic forces, Biochim. Biophys. Acta. 1373 (1998) 112–118.

[6] E. London, D.A. Brown, Insolubility of lipids in triton X-100: physical origin and relationship to sphingolipid/cholesterol membrane domains (rafts), Biochim. Biophys. Acta. 1508 (2000) 182–195.

[7] R. Schroeder, E. London, D.A. Brown, Interactions between saturated acyl chains confer detergent resistance on lipids and glycosylphosphatidylinositol (GPI)-anchored proteins: GPI-anchored proteins in liposomes and cells show similar behavior, Proc. Natl. Acad. Sci. USA. 91 (1994) 12130–12134.

[8] M.R. Vist, J.H. Davis, Phase equilibria of cholesterol/dipalmitoylphosphatidylcholine mixtures: 2H nuclear magnetic resonance and differential scanning calorimetry, Biochemistry 29 (1990) 451–464.

[9] M.B. Sankaram, T.E. Thompson, Interaction of cholesterol with various glycerophospholipids and sphingomyelin, Biochemistry 29 (1990) 10670–10675.

[10] M.B. Sankaram, T.E. Thompson, Cholesterol-induced fluid-phase immiscibility in membranes, Proc. Natl. Acad. Sci. USA. 88 (1991) 8686–8690.

[11] C.R. Mateo, A.U. Acuna, J.C. Brochon, Liquid-crystalline phases of cholesterol/lipid bilayers as revealed by the fluorescence of trans-parinaric acid, Biophys. J. 68 (1995) 978–987.

[12] T.P. McMullen, R.N. McElhaney, New aspects of the interaction of cholesterol with dipalmitoylphosphatidylcholine bilayers as revealed by high-sensitivity differential scanning calorimetry, Biochim. Biophys. Acta 1234 (1995) 90–98.

[13] D.A. Brown, J.K. Rose, Sorting of GPI-anchored proteins to glycolipid-enriched membrane subdomains during transport to the apical cell surface, Cell 68 (1992) 533–544.

[14] M. Ge, K.A. Field, R. Aneja, D. Holowka, B. Baird, J.H. Freed, Electron spin resonance characterization of liquid ordered phase of detergent-resistant membranes from RBL-2H3 cells, Biophys. J. 77 (1999) 925–933.

[15] A.G. Ostermeyer, B.T. Beckrich, K.A. Ivarson, K.E. Grove, D.A. Brown, Glycosphingolipids are not essential for formation of detergent-resistant membrane rafts in melanoma cells. methyl-beta-cyclodextrin does not affect cell surface transport of a GPI-anchored protein, J. Biol. Chem. 274 (1999) 34459–34466.

[16] A. Radhakrishnan, H.M. McConnell, Condensed complexes of cholesterol and phospholipids, Biophys. J. 77 (1999) 1507–1517.

[17] A. Radhakrishnan, H.M. McConnell, Chemical activity of cholesterol in membranes, Biochemistry 39 (2000) 8119–8124.

[18] P.F. Almeida, W.L. Vaz, T.E. Thompson, Percolation and diffusion in three-component lipid bilayers: effect of cholesterol on an equimolar mixture of two phosphatidylcholines, Biophys. J. 64 (1993) 399–412.

[19] J.R. Silvius, D. del Giudice, M. Lafleur, Cholesterol at different bilayer concentrations can promote or antagonize lateral segregation of phospholipids of differing acyl chain length, Biochemistry 35 (1996) 15198–15208.

[20] T.Y. Wang, R. Leventis, J.R. Silvius, Fluorescence-based evaluation of the partitioning of lipids and lipidated peptides into liquid-ordered lipid microdomains: a model for molecular partitioning into ‘lipid rafts’, Biophys. J. 79 (2000) 919–933.

[21] R.J. Schroeder, S.N. Ahmed, Y. Zhu, E. London, D.A. Brown, Cholesterol and sphingolipid enhance the Triton X-100 insolubility of glycosylphosphatidylinositol-anchored proteins by promoting the formation of detergent-insoluble ordered membrane domains, J. Biol. Chem. 273 (1998) 1150–1157.

[22] X. Xu, E. London, The effect of sterol structure on membrane lipid domains reveals how cholesterol can induce lipid domain formation, Biochemistry 39 (2000) 843–849.

[23] P.L. Yeagle, J.E. Young, Factors contributing to the distribution of cholesterol among phospholipid vesicles, J. Biol. Chem. 261 (1986) 8175–8181.

[24] P. Mattjus, J.P. Slotte, Does cholesterol discriminate between sphingomyelin and phosphatidylcholine in mixed monolayers containing both phospholipids?, Chem. Phys. Lipids. 81 (1996) 69–80.

[25] T.P. McMullen, R.N. Lewis, R.N. McElhaney, Differential scanning calorimetric study of the effect of cholesterol on the thermotropic phase behavior of a homologous series of linear saturated phosphatidylcholines, Biochemistry 32 (1993) 516–522.
[26] A. Kusumi, W.K. Subczynski, M. Pasenkiewicz-Gierula, J.S. Hyde, H. Merkle, Spin-label studies on phosphatidylcholine-cholesterol membranes: effects of alkyl chain length and unsaturation in the fluid phase, Biochim. Biophys. Acta 854 (1986) 307–317.
[27] A. Kusumi, M. Pasenkiewicz-Gierula, Rotational diffusion of a steroid molecule in phosphatidylcholine membranes: effects of alkyl chain length, unsaturation, and cholesterol as studied by a spin-label method, Biochemistry 27 (1988) 4407–4415.
[28] M. Pasenkiewicz-Gierula, W.K. Subczynski, A. Kusumi, Rotational diffusion of a steroid molecule in phosphatidylcholine-cholesterol membranes: fluid-phase microimmiscibility in unsaturated phosphatidylcholine-cholesterol membranes, Biochemistry 29 (1990) 4059–4069.
[29] W.K. Subczynski, W.E. Antholine, J.S. Hyde, A. Kusumi, Microimmiscibility and three-dimensional dynamic structures of phosphatidylcholine-cholesterol membranes: translational diffusion of a copper complex in the membrane, Biochemistry 29 (1990) 7936–7945.
[30] Y.K. Shin, J.H. Freed, Dynamic imaging of lateral diffusion by electron spin resonance and study of rotational dynamics in model membranes. Effect of cholesterol, Biophys. J. 55 (1989) 537–550.
[31] Y.K. Shin, J.K. Moscicki, J.H. Freed, Dynamics of phosphatidylcholine-cholesterol mixed model membranes in the liquid crystalline state, Biophys. J. 57 (1990) 445–459.
[32] D.C. Mitchell, B.J. Litman, Effect of cholesterol on molecular order and dynamics in highly polyunsaturated phospholipid bilayers, Biophys. J. 75 (1998) 896–908.
[33] J.P. Hagen, H.M. McConnell, Liquid–liquid immiscibility in lipid monolayers, Biochim. Biophys. Acta 1329 (1997) 7–11.
[34] F. Rodriguez, J.F. Tocanne, A. Lopez, Self-association processes involving anthracene labeled phosphatidylcholines in model membrane, Biophys. Chem. 53 (1995) 169–180.
[35] S. Mazères, B. Lagane, M. Welby, V. Trégou, A. Lopez, Probing the lateral organization of membranes: Fluorescence repercussions of pyrene probe distribution, Spectrochim. Acta A 57 (2001) 2297–2311.
[36] P.F. Almeida, W.L.C. Vaz, T.E. Thompson, Lateral diffusion in the liquid phases of dimyristoylphosphatidylcholine/cholesterol lipid bilayers: a free volume analysis, Biochemistry 31 (1992) 6739–6747.
[37] C.W. McClare, An accurate and convenient organic phosphorus assay, Anal. Biochem. 39 (1971) 527–530.
[38] G. Duportail, P. Lianos, Vesicles, fluorescence probing of vesicles using pyrene and pyrene derivatives, in: M. Rosoff (Ed.), Surfactant Science Series (New York), 62, 1996, p. 295.
[39] R.V. Todesco, R.A. Basheer, P.V. Kamat, Photophysical and photochemical behavior of poly(1-vinylpyrene). Evidence for dual excimer fluorescence, Macromolecules 19 (1986) 2390–2397.
[40] W.K. Subczynski, A. Wisniewski, J.J. Yin, J.S. Hyde, A. Kusumi, Hydrophobic barriers of lipid bilayer membranes formed by reduction of water penetration by alkyl chain unsaturation and cholesterol, Biochemistry 33 (1994) 7670–7681.
[41] D.C. Dong, M.A. Winnik, The Py scale of solvent polarities. Solvent effects on the vibronic fine structure of pyrene fluorescence and empirical correlations with ET and *Y* values, Photochem. Photobiol. 35 (1982) 17–21.
[42] T. Rog, M. Pasenkiewicz-Gierula, Cholesterol effects on the phospholipid condensation and packing in the bilayer: a molecular simulation study, FEBS Letters 502 (2001) 68–71.
[43] F. Jahnig, Critical effects from lipid-protein interaction in membranes. I. Theoretical description, Biophys. J. 36 (1981) 329–345.
[44] M.M. Sperotto, O.G. Mouritsen, Monte Carlo simulation studies of lipid order parameter profiles near integral membrane proteins, Biophys. J. 59 (1991) 261–270.
[45] P.F. Almeida, W.L. Vaz, T.E. Thompson, Lateral diffusion and percolation in two-phase, two-component lipid bilayers. Topology of the solid-phase domains in-plane and across the lipid bilayer, Biochemistry 31 (1992) 7198–7210.
[46] V. Schram, J.F. Tocanne, A. Lopez, Influence of obstacles on lipid lateral diffusion: computer simulation of FRAP experiments and application to proteoliposomes and biomembranes, Eur. Biophys. J. 23 (1994) 337–348.
[47] R.A. Demel, K.R. Bruckdorfer, L.L. van Deenen, Structural requirements of sterols for the interaction with lecithin at the air water interface, Biochim. Biophys. Acta 255 (1972) 311–320.
[48] E.K. Fridriksson, P.A. Shipkova, E.D. Sheets, D. Holowka, B. Baird, F.W. McLafferty, Quantitative analysis of phospholipids in functionally important membrane domains from RBL-2H3 mast cells using tandem high-resolution mass spectrometry, Biochemistry 38 (1999) 8056–8063.
[49] B. Lagane, G. Gaibelet, E. Meilhoc, J.M. Masson, L. Cézanne, A. Lopez, Role of sterols in modulating the human mu-opioid receptor function in saccharomyces cerevisiae, J. Biol. Chem. 275 (2000) 33197–33200.
[50] K. Burger, G. Gimpl, F. Fahrenholz, Regulation of receptor function by cholesterol, Cell. Mol. Life Sci. 57 (2000) 1577–1592.
[51] M. Pasenkiewicz-Gierula, Y. Takaoka, H. Miyagawa, K. Kitamura, A. Kusumi, Charge pairing of headgroups in phosphatidylcholine membranes: a molecular dynamics simulation study, Biophys. J. 76 (1999) 1228–1240.

[52] B.A. Lewis, D.M. Engelman, Lipid bilayer thickness varies linearly with acyl chain length in fluid phosphatidylcholine vesicles, J. Mol. Biol. 166 (1983) 211–217.
[53] S.W. Chiu, E. Jakobsson, S. Subramaniam, H.L. Scott, Combined monte carlo and molecular dynamics simulation of fully hydrated dioleyl and palmitoyl-oleyl phosphatidylcholine lipid bilayers, Biophys. J. 77 (1999) 2462–2469.
[54] S. Tristram-Nagle, H.I. Petrache, J.F. Nagle, Structure and interactions of fully hydrated dioleoylphosphatidylcholine bilayers, Biophys. J. 75 (1998) 917–925.